Mott metal-insulator transition in the half-filled Hubbard model on the triangular lattice

Massimo Capone, Luca Capriotti, and Federico Becca
International School for Advanced Studies (SISSA), and Istituto Nazionale per la Fisica della Materia (INFM), Unità Trieste-SISSA, Via Beirut 2-4, I-34014 Trieste, Italy

Sergio Caprara
Dipartimento di Fisica, Università di Roma ''La Sapienza,'' and Istituto Nazionale per la Fisica della Materia (INFM), Unità Roma 1, Piazzale Aldo Moro 2, I-00185 Roma, Italy

(Received 20 June 2000; published 2 February 2001)

We investigate the metal-insulator transition in the half-filled Hubbard model on the two-dimensional triangular lattice using both the Kotliar-Ruckenstein slave-boson technique and an exact numerical diagonalization of finite clusters. Contrary to the case of a square lattice, where a perfect nesting of the Fermi surface leads to a metal-insulator transition at arbitrarily small values of U, always accompanied by antiferromagnetic ordering, on a triangular lattice, due to the lack of perfect nesting, the transition takes place at a finite value of U, and frustration induces a nontrivial competition among different magnetic phases. Indeed, within the mean-field approximation in the slave-boson approach, as the interaction grows the paramagnetic metal turns into a metallic phase with incommensurate spiral ordering. Increasing the interaction further, a linear spin-density wave is stabilized, and finally for strong coupling the latter phase undergoes a first-order transition toward an antiferromagnetic insulator. No trace of the intermediate phases is seen in the exact diagonalization results, indicating a transition between a paramagnetic metal and an antiferromagnetic insulator.

DOI: 10.1103/PhysRevB.63.085104 PACS number(s): 71.10.Fd, 71.30.+h, 75.10.Lp

The Mott metal-insulator transition (MIT), i.e., the transition from a metallic to an insulating phase driven by electronic correlation,[1,2] is one of the most relevant issues in condensed-matter theory. In the last few years it has also been the object of intensive study, due to the considerable experimental evidence of Mott insulators ranging from the parent compounds of the superconducting cuprates[3] to the alkali fullerides of the type A_4C_{60}.[4]

The simplest model in which the competition between the delocalizing effect of the kinetic energy and the electronic correlation can give rise to a MIT is the Hubbard model

$$\mathcal{H}=-t\sum_{\langle ij\rangle\sigma}(c^{\dagger}_{i,\sigma}c_{j,\sigma}+\text{H.c.})-\mu\sum_{i,\sigma}c^{\dagger}_{i,\sigma}c_{i,\sigma}+U\sum_{i}n_{i\uparrow}n_{i\downarrow}, \tag{1}$$

where $c^{\dagger}_{i,\sigma}(c_{i,\sigma})$ creates (destroys) an electron with spin σ on site i, and $n_{i,\sigma}=c^{\dagger}_{i,\sigma}c_{i,\sigma}$ is the number operator; t is the hopping amplitude, U is the Hubbard on-site repulsion, and μ is the chemical potential. The hopping is restricted to nearest neighbors, and the indices i and j label the points $\mathbf{R}_i$ and $\mathbf{R}_j$ of a d-dimensional lattice.

At half-filling (i.e., for a number of electrons equal to the number of sites), this model is known to undergo a MIT by increasing the interaction strength U. On a d-dimensional cubic lattice the perfect nesting property of the Fermi surface makes the model unstable toward antiferromagnetism as soon as a nonzero U is turned on, driving the system to an insulating state. In this paper we focus on a triangular lattice in $d=2$ as a prototype for a model where perfect nesting is absent for the uncorrelated metal.[5] Since in the $U/t\to\infty$ (Heisenberg) limit the model is likely to display a Néel-ordered (insulating) ground state (GS),[6,7] a MIT is expected to occur for finite U.

Besides its theoretical relevance, our analysis has also an experimental counterpart. In fact, adlayer structures on semiconductor surfaces, such as SiC(0001) (Ref. 8) or K/Si(111):B,[9] recently turned out to be almost ideal environments for the study of Mott insulators,[10] and are characterized by a $\sqrt{3}\times\sqrt{3}$ arrangement of the dangling-bond surface orbitals, which are likely to be well described by two-dimensional strongly correlated Hamiltonians[10] on a triangular lattice.

Hartree-Fock (HF) calculations, performed by Krishnamurthy and co-workers,[11,12] produce a rather rich phase diagram: for small U the system is a paramagnetic metal (PM), which turns to a metal with incommensurate spiral spin-density wave (spiral metal, SM) at $U=U_{c1}=3.97t$. Two successive first-order transitions occur, further increasing the coupling: at $U=U_{c2}=4.45t$ a semimetallic linear spin-density wave (LSDW) is stabilized, and a first-order MIT to an antiferromagnetic insulator (AFMI) occurs at $U=U_{c3}=5.27t$. In the same work it was also argued that at finite temperature the model should present a Mott transition between a paramagnetic metal and a paramagnetic insulator.

However, the above transitions only occur at relatively large U/t and the HF approximation is unreliable in the intermediate- and strong-coupling regimes, as it gives a linear dependence of the PM energy on U, and overestimates the tendency toward the AFMI, stable in the strong-coupling limit. Conversely, the slave-boson (SB) approach[13,14] leads to a lower energy for finite U/t in the PM phase, reducing to the HF limit for $U/t\to 0$, and correctly reproduces the GS energy proportional to t^2/U in the limit $U\to\infty$. Therefore, we adopt the more appropriate SB approach as an interpolating scheme between the $U/t=0$ and $U/t\to\infty$ regimes. To allow for the presence of incommensurate spiral spin order-

ing, we introduce the spin-rotational invariant formulation[15] of the Kotliar-Ruckenstein SB approach.[14] The reader can find further details in Ref. 15.

On each site we introduce a set of four SB operators e_i, $s_{i,\uparrow}$, $s_{i,\downarrow}$, and d_i to label empty (e), singly (s), and doubly (d) occupied sites, respectively. The spin projection $\mathfrak{s}=\uparrow,\downarrow$ is measured with respect to a local quantization axis, which is allowed to vary from site to site. The resulting SB Hamiltonian is

$$\mathcal{H}=-t\sum_{\substack{\langle ij\rangle\\ \mathfrak{s},\mathfrak{s}'}}[\tilde{c}^{\dagger}_{i,\mathfrak{s}}z^{\dagger}_{i,\mathfrak{s}}(\mathcal{R}^{\dagger}_i\mathcal{R}_j)_{\mathfrak{s},\mathfrak{s}'}z_{j,\mathfrak{s}'}\tilde{c}_{j,\mathfrak{s}'}+\mathrm{H.c.}]$$
$$-\mu\sum_{i,\mathfrak{s}}\tilde{c}^{\dagger}_{i,\mathfrak{s}}\tilde{c}_{i,\mathfrak{s}}+U\sum_i d^{\dagger}_i d_i+\sum_i \lambda_i\Big(e^{\dagger}_i e_i+d^{\dagger}_i d_i$$
$$+\sum_{\mathfrak{s}} s^{\dagger}_{i,\mathfrak{s}}s_{i,\mathfrak{s}}-1\Big)+\sum_{i,\mathfrak{s}}\Lambda_{i,\mathfrak{s}}(\tilde{c}^{\dagger}_{i,\mathfrak{s}}\tilde{c}_{i,\mathfrak{s}}-s^{\dagger}_{i,\mathfrak{s}}s_{i,\mathfrak{s}}-d^{\dagger}_i d_i), \tag{2}$$

where $\tilde{c}_{i,\mathfrak{s}}$ and $\tilde{c}^{\dagger}_{i,\mathfrak{s}}$ are the pseudofermion operators, the Lagrange multipliers λ_i and $\Lambda_{i,\mathfrak{s}}$ enforce on each site the completeness constraint and the correct fermion counting respectively, the operator $\mathcal{R}_i$ rotates the local reference frame back to the laboratory frame, and the operator

$$z_{i,\mathfrak{s}}=\frac{e^{\dagger}_i s_{i,\mathfrak{s}}+s^{\dagger}_{i,-\mathfrak{s}}d_i}{\sqrt{1-d^{\dagger}_i d_i-s^{\dagger}_{i,\mathfrak{s}}s_{i,\mathfrak{s}}}\sqrt{1-e^{\dagger}_i e_i-s^{\dagger}_{i,-\mathfrak{s}}s_{i,-\mathfrak{s}}}}$$

reconstructs the hopping amplitude in the enlarged Fock space, and yields the correct $U\to 0$ limiting behavior in the mean-field approximation.[14,15] When the angle between two local quantization axes depends only on their relative position, up to a global phase factor one can assume $\mathcal{R}^{\dagger}_i\mathcal{R}_j=\exp[i\mathbf{Q}\cdot(\mathbf{R}_i-\mathbf{R}_j)\tau_y/2]$, where τ_y is the Pauli matrix and $\mathbf{Q}$ is the (incommensurate) modulating wave vector.[15] In such a case a mean-field description with real site-independent expectation values for the SB operators,

$$\langle e^{(\dagger)}_i\rangle=e_0,\quad \langle s^{(\dagger)}_{i,\mathfrak{s}}\rangle=s_{0,\mathfrak{s}},\quad \langle d^{(\dagger)}_i\rangle=d_0, \tag{3}$$

and for the Lagrange multipliers,

$$\langle\lambda_i\rangle=\lambda_0,\quad \langle\Lambda_{i,\mathfrak{s}}\rangle=\Lambda_{0,\mathfrak{s}}, \tag{4}$$

is possible. Equations (3) and (4) refer to the case in which the translational symmetry is not broken and the expectation values of the bosons and of the Lagrange multipliers do not depend on the site. We have also studied configurations with broken translational symmetry. In particular, we considered solutions in which in the bosons have different values on each of the three sublattices, and analogous to the LSDW found within the HF approximation.[12] The latter solutions can be found considering a four-site unit cell. A similar SB calculation was performed in Ref. 16, where, however, the generalization of the SM phase found in the HF approximation was never recovered as an energy minimum. In the case of spiral spin ordering, Hamiltonian (2) can be analytically diagonalized by adopting the Bloch representation, and performing a unitary transformation with respect to spin indices, yielding

$$E_{\mathbf{k},\pm}=\frac{1}{2}[t(z^2_{0,\uparrow}+z^2_{0,\downarrow})T_e+\Lambda_{0,\uparrow}+\Lambda_{0,\downarrow}]-\mu$$
$$\pm\frac{1}{2}\sqrt{[t(z^2_{0,\uparrow}-z^2_{0,\downarrow})T_e+\Lambda_{0,\uparrow}-\Lambda_{0,\downarrow}]^2+4t^2z^2_{0,\uparrow}z^2_{0,\downarrow}T^2_o},$$

where $T_e=-\Sigma_{\mathbf{l}}\cos(\mathbf{Q}\cdot\mathbf{l}/2)\cos(\mathbf{k}\cdot\mathbf{l})$, $T_o=-\Sigma_{\mathbf{l}}\sin(\mathbf{Q}\cdot\mathbf{l}/2)\sin(\mathbf{k}\cdot\mathbf{l})$, and $\mathbf{l}=(1,0),(1/2,\pm\sqrt{3}/2)$ are the nearest-neighbor displacements. The self-consistency equations are obtained by minimizing the free energy

$$\mathcal{F}=\mathcal{F}_0-T\sum_{\mathbf{k},\alpha=\pm}\log(1+e^{-E_{\mathbf{k},\alpha}/T}),$$

where $\mathcal{F}_0=N[Ud^2_0+\lambda_0(e^2_0+d^2_0+s^2_{0,\uparrow}+s^2_{0,\downarrow}-1)-\Lambda_{0,\uparrow}(d^2_0+s^2_{0,\uparrow})-\Lambda_{0,\downarrow}(d^2_0+s^2_{0,\downarrow})+\mu n]$, N is the number of sites, and n is the electron density per site, and read

$$\frac{\partial\mathcal{F}_0}{\partial\mathcal{X}}+\sum_{\mathbf{k},\alpha=\pm}\frac{\partial E_{\mathbf{k},\alpha}}{\partial\mathcal{X}}f(E_{\mathbf{k},\alpha})=0, \tag{5}$$

where $f(E)=[e^{E/T}+1]^{-1}$ is the Fermi function and $\mathcal{X}$ represents generically one of the parameters (3) and (4) and the two components of the pitch vector $\mathbf{Q}$. The chemical potential μ is fixed by the condition

$$\sum_{\mathbf{k},\alpha=\pm}f(E_{\mathbf{k},\alpha})=nN.$$

In this paper we henceforth assume $n=1$ (half-filling).

The self-consistency equations (5) yield the same solutions found in the HF approximation, namely, a paramagnetic metal, a metal with incommensurate spiral ordering, a linear spin-density wave and an antiferromagnetic insulator. As in the HF method, the PM-SM transition is continuous, and the other two transitions are of first order, but all of them occur at larger coupling values: $U_{c1}=6.68t$, $U_{c2}=6.84t$, and $U_{c3}=7.68t$. The energy curves corresponding to the above phases are reported in Fig. 1. Our results agree with Ref. 16 as far as the PM, AFMI, and LSDW phases are concerned, but we also find a region of stability for the SM phase, which was not detected in Ref. 16. These authors were indeed looking for spiral phases starting from the strong-coupling side, and following them to weaker coupling. On the other hand, our analysis shows that a spiral phase develops continuously from the PM at intermediate coupling, and ends in a critical point soon after the level crossing with the AFMI (see the inset in Fig. 1), and does not exist at strong coupling. Therefore, our SM phase is the generalization of the corresponding phase found within the HF approximation,[12] and it is unrelated to the high-energy SM phases of Ref. 16. However, the region of existence of the SM is narrower within the SB method as compared to the HF method, and the magnetization $m=\frac{1}{2}(n_\uparrow-n_\downarrow)$ is always less than 0.1, and stays smaller

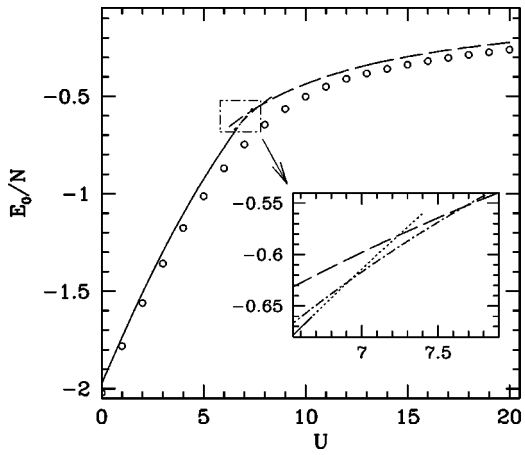

FIG. 1. U dependence of the ground-state energy per site. SB results: PM (solid line), SM (dotted line), LSDW (dot-dashed line), and AFMI (dashed line). Open dots are the exact diagonalization results for the $N=12$ cluster.

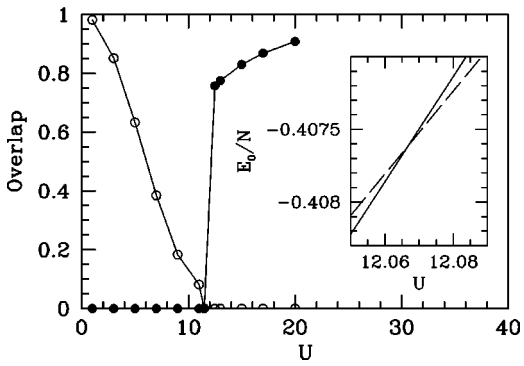

FIG. 2. Overlap of the finite-U GS with the $U=0$ (empty dots) and the $U=100t$ (full dots) GS's, for $N=12$. In the inset the GS energy per site in the $\mathbf{k}=(0,0)$ (solid line) and $\mathbf{k}=(2\pi/3,0)$ (dashed line) subspaces is plotted vs U.

than the HF value ($\lesssim 0.4$). Therefore the jump of the magnetization at the SM-AFMI transition is substantially larger than in the HF approximation. We point out that, contrary to nesting models, where the presence of free particles (doping) is a necessary condition for spiral ordering,[15,17,18] here the spiral phase exists at half-filling, as previously shown in Ref. 11, within the HF approximation. Despite the overall qualitative agreement between the HF and SB phase diagrams, the main outcome of a comparison between them is that the stability of the SM phase is strongly reduced. Furthermore, the SM is hardly distinguishable from the PM in its whole region of stability. It is therefore reasonable to expect that the inclusion of quantum fluctuations washes out these phases which are characterized by small order parameters and are very close in energy both to the PM and the AFMI (see the inset in Fig. 1). On the other hand, the PM phase at small U/t reduces asymptotically to the exact solution, and should be slightly affected at larger values. The AFMI phase at large U/t is robust, and the only effect of quantum fluctuations is expected to be a reduction of the sublattice magnetization with respect to saturation (cf. the case of the Heisenberg model[7]). This leaves the way open for a direct Mott transition between the PM and the AFMI.

Despite the strong frustration of the antiferromagnetic (AFM) order on the triangular lattice,[6,7] both the HF and SB approaches indicate no paramagnetic Mott insulating phase in the zero-temperature phase diagram of the half-filled Hubbard model. In particular, within the SB approach, we can indicate how far the system is from the Brinkman-Rice transition[2] to a paramagnetic Mott insulator. In fact, if the possibility for magnetic ordering is neglected, the paramagnetic metallic phase undergoes a Brinkman-Rice transition with vanishing double occupancy and an effective hopping amplitude, for a critical value (at $T=0$) of the Hubbard interaction $U_{BR}=32tN^{-1}\Sigma_{\mathbf{k}}\varepsilon_{\mathbf{k}}\Theta(2t\varepsilon_{\mathbf{k}}+\mu)$ $[\varepsilon_{\mathbf{k}}=-T_e(\mathbf{Q}=0),\mu/t=-0.835]$,[2,14] i.e., $U_{BR}/t\simeq 15.8$ on the triangular lattice. As we see, this value is much larger than U_{c1}/t, U_{c2}/t and U_{c3}/t found above. The system is therefore not even close to the Brinkman-Rice transition when a MIT occurs.

In order to understand to what extent the picture we found within the mean-field SB theory survives in an exact treatment of the model, we performed an exact diagonalization of small clusters by means of the standard Lanczos algorithm. The largest lattice compatible with all the symmetries of the model that can be handled with exact diagonalization is a $N=12$ site cluster.[6] It is clear that, despite the exact determination of the GS energy and wave function, the exact diagonalization results suffer from finite-size effects, and that no reliable size scaling is possible for the present problem. We point out, however, that the AFMI has a wide gap in the single-particle spectrum, and is well described by small clusters. This is not the case for the incommensurate phases found above within the SB approach. Therefore we expect that exact diagonalization should characterize properly the Mott transition toward the AFMI, while it could miss the appearance of the SM and the LSDW. Finite-size calculations are reliable only if the number of electrons corresponds to a closed-shell configuration. Since 12 electrons on 12 sites are not a closed-shell configuration for periodic or antiperiodic boundary conditions, we always used twisted boundary conditions with a suitable phase such that the half-filled system is in a closed-shell configuration. This is important in order to perform a reasonable investigation of the conduction properties of a finite-size system. It turns out that the boundary conditions that minimize the energy in a closed-shell configuration for $U=0$ leave the system in a closed-shell configuration at all U. The energy is shown as a function of U in Fig. 1. The overall agreement with the mean-field SB results is good, the largest deviations ($\sim 20\%$) being, as expected, at intermediate coupling ($U/t\sim 7$).

To check the occurrence of a discontinuous phase transition we evaluated the overlap between the GS wave function and the two limiting cases of $U=0$, and for large U (namely, $U=100t$). As shown in Fig. 2, on the large-U side of the diagram the GS has a large overlap to the AFM strong-coupling state, and a vanishing overlap with the noninteracting metallic one. On the metallic side the overlap with the noninteracting state is always finite, but it is a decreasing

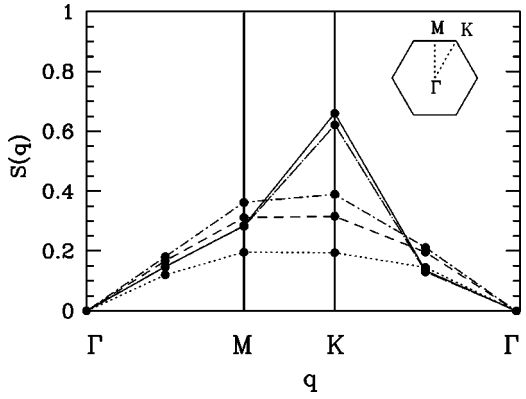

FIG. 3. Spin structure factor $S(\mathbf{q})$: $U=2t$ (dotted line), $U=8t$ (dashed line), $U=11.5t$ (dot-short-dashed line), $U=12.5t$ (dot-long-dashed line), and $U=40t$ (solid line).

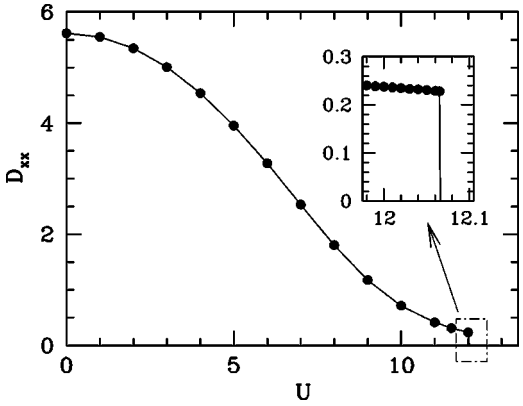

FIG. 4. Exact calculation of the Drude weight as a function of U for the $N=12$ cluster.

function of U; in this regime the GS has a vanishing overlap with the AFM state. We therefore have clear evidence of a strongly correlated metal with a decreasing coherent part. In particular the sharp change of the GS wave function at $U_{MIT}\simeq 12.07t$ is due to a level crossing occurring between metallic and antiferromagnetic solutions, as shown in the inset of Fig. 2. These results, however, do not rule out the possibility of a continuous transition within the metallic phase, i.e. the PM-SM transition found with SB.

In Fig. 3 we show the spin structure factor $S(\mathbf{q})=\Sigma_{i,j}S_i^zS_j^z\exp[\mathbf{q}\cdot(\mathbf{R}_i-\mathbf{R}_j)]/N$ for different values of U. The results do not suggest any intermediate state between a metallic state without magnetic order and the AFM insulator, as $S(\mathbf{q})$ abruptly changes from a structureless behavior to an AFM pattern peaked at the classical ordering wave vector, i.e., $\mathbf{Q_0}=(4\pi/3,0)$. Although we suspect that the intermediate phases are artifacts of the mean-field approach, the weakness and the strong size dependence of the spiral phases suggested by the SB results may make them unaccessible on our 12-site lattice.

Using the Lanczos algorithm we have also calculated the finite-frequency optical conductivity $\sigma(\omega)$ and the Drude weight, measuring the electronic mobility. The real part of the xx component of the conductivity tensor for a tight-binding model at zero temperature may be expressed in terms of the Kubo formula[19]

$$\sigma_{xx}(\omega)=D_{xx}\delta(\omega)+\mathrm{Im}\left\langle \phi_0\left| J_x^{\dagger}\frac{1}{\omega-\mathcal{H}+E_0-i\delta}J_x\right|\phi_0\right\rangle, \tag{6}$$

where $J_x=\Sigma_{i,\sigma,\mathbf{l}}l_x(c_{i,\sigma}^{\dagger}c_{i+\mathbf{l},\sigma}-\mathrm{H.c.})$ is the x component of the current operator, and l_x are the x components of the nearest-neighbor displacement vectors $\mathbf{l}$ defined above. The coefficient of the zero-frequency delta function contribution D_{xx}, the Drude weight, is given by the f sumrule[19]

$$D_{xx}=-\frac{\pi e^2}{2}\langle\mathcal{H}_x^t\rangle-\sum_{n\neq 0}\frac{|\langle\phi_0|J_x|\phi_n\rangle|^2}{E_n-E_0}, \tag{7}$$

where $\mathcal{H}_x^t=\Sigma_{i,\sigma,\mathbf{l}}l_x^2(c_{i,\sigma}^{\dagger}c_{i+\mathbf{l},\sigma}+\mathrm{H.c.})$, and $|\phi_n\rangle$ is the eigenfunction of $\mathcal{H}$ with eigenvalue E_n.

The latter quantity, which is reported in Fig. 4, is a direct measure of the metallic character of the state, and the MIT is signaled by the vanishing of D_{xx}.[20] For a finite system, D_{xx} does not vanish for any value of U. For $U<U_{MIT}$, D_{xx} is a decreasing function of the interaction, which resembles the overlap in Fig. 2. An abrupt change takes place at the level-crossing point, and for $U>U_{MIT}$ it becomes negative, a common phenomenon in the insulating phase of a small-size system.[21]

All the results of exact diagonalization point in the same direction: the metal-AFMI level crossing found within the SB mean-field approach is shifted to larger values of U. The metallic solution exhibits a continuous loss of metallicity with increasing U. The Drude weight is finite up to the MIT on the 12-site lattice, although it is quite small (4% of the noninteracting value). We remark that, due to finite-size effects, we cannot exclude the possibility that D_{xx} vanishes before the transition to the AFMI is reached. In such a case, there would be a region of parameters in which the paramagnetic insulator exist, though the SB results point in the opposite direction.

In conclusion, using the slave-boson technique and the exact diagonalization, we have investigated the zero-temperature phase diagram of the half-filled Hubbard model on a two dimensional triangular lattice. The mean-field SB approach displays a rich phase diagram which qualitatively resembles the one from HF calculations, but, on the other hand, drastically reduces the stability of the spiral metal and of the linear spin-density-wave states. That is, the weak-coupling paramagnetic metal continuously evolves into a spiral metal at $U=U_{c1}=6.68t$, which crosses the linearly polarized spin-density-wave ground state at $U=U_{c2}=6.84t$. The latter phase undergoes a further first-order transition toward an antiferromagnetic insulator at $U=U_{c3}=7.68t$. All these transitions occur for coupling constants substantially smaller than the critical value for the Brinkman-Rice transition to a paramagnetic insulator ($U_{BR}=15.8t$). The exact-diagonalization results present a first-order transition

between the paramagnetic metal and the antiferromagnetic insulator at $U_{MIT}=12.07t$, without intermediate ''exotic'' phases.

It is a pleasure to thank S. Sorella and A. Parola for suggestions and fruitful discussions. Useful communications with A. E. Trumper are also acknowledged. S. C. acknowledges the kind hospitality of the International School for Advanced Studies in Trieste, where most of this work was carried out. This work was partially supported by MURST (COFIN99).

[1] N. F. Mott, *Metal-Insulator Transitions* (Taylor and Francis, London, 1974); A. Georges, G. Kotliar, W. Krauth, and M.J. Rozenberg, Rev. Mod. Phys. **68**, 13 (1996).
[2] W.F. Brinkman and T.M. Rice, Phys. Rev. B **2**, 4302 (1970).
[3] Y.J. Uemura, W.J. Kossler, X.H. Yu, J.R. Kempton, H.E. Schone, D. Opie, C.E. Stronach, D.C. Johnston, M.S. Alvarez, and D.P. Goshorn, Phys. Rev. Lett. **59**, 1045 (1987); J.M. Tranquada, D.E. Cox, W. Kunnmann, H. Moudden, G. Shirane, M. Suenaga, P. Zolliker, D. Vaknin, S.K. Sinha, M.S. Alvarez, A.J. Jacobson, and D.C. Johnston, *ibid.* **60**, 156 (1988).
[4] M. Capone, M. Fabrizio, P. Giannozzi, and E. Tosatti, Phys. Rev. B **62**, 7619 (2000).
[5] E. Tosatti and P.W. Anderson, Solid State Commun. **14**, 773 (1974).
[6] B. Bernu, C. Lhuillier, and L. Pierre, Phys. Rev. Lett. **69**, 2590 (1992); B. Bernu, P. Lecheminant, C. Lhuillier, and L. Pierre, Phys. Rev. B **50**, 10 048 (1994).
[7] L. Capriotti, A.E. Trumper, and S. Sorella, Phys. Rev. Lett. **82**, 3899 (1999); A.E. Trumper, L. Capriotti, and S. Sorella, Phys. Rev. B **61**, 11529 (2000).
[8] L.I. Johansson, F. Owman, and P. Mårtensjon, Surf. Sci. **360**, L478 (1996); J.-M. Themlin, I. Forbeaux, V. Langlais, H. Belkhir, and J.-M. Debever, Europhys. Lett. **39**, 61 (1997).
[9] H.H. Weitering, X. Shi, P.D. Johnson, J. Chen, N.J. DiNardo, and K. Kempa, Phys. Rev. Lett. **78**, 1331 (1997).
[10] C.S. Hellberg and S.C. Erwin, Phys. Rev. Lett. **83**, 1003 (1999); G. Santoro, S. Sorella, F. Becca, S. Scandolo, and E. Tosatti, Surf. Sci. **402**, 802 (1998).
[11] H.R. Krishnamurthy, C. Jayaprakash, S. Sarker, and W. Wenzel, Phys. Rev. Lett. **64**, 950 (1990).
[12] C. Jayaprakash, H.R. Krishnamurthy, S. Sarker, and W. Wenzel, Europhys. Lett. **15**, 625 (1991).
[13] S.E. Barnes, J. Phys. F: Met. Phys. **6**, 1375 (1976); N. Read and D. Newns, J. Phys. C **16**, 3273 (1983); P. Coleman, Phys. Rev. B **29**, 3035 (1984).
[14] G. Kotliar and A.E. Ruckenstein, Phys. Rev. Lett. **57**, 1362 (1986).
[15] E. Arrigoni and G.C. Strinati, Phys. Rev. B **44**, 7455 (1991).
[16] C.J. Gazza, A.E. Trumper, and H.A. Ceccatto, J. Phys.: Condens. Matter **6**, L625 (1994).
[17] V. V. Tugushev, in *Electronic Phase Transitions*, edited by W. Hanke and Yu. Kopaev (Elsevier, Amsterdam, 1992), p. 237, and references therein.
[18] S. Caprara, M. Avignon, and V. Tugushev, Phys. Lett. A **255**, 98 (1999).
[19] F.P. Maldague, Phys. Rev. B **16**, 2437 (1977).
[20] W. Kohn, Phys. Rev. **133**, A171 (1964).
[21] E. Dagotto, Rev. Mod. Phys. **66**, 763 (1994).